Anomalous diffusion in two-dimensional Euclidean and prefractal geometrical models of heterogeneous porous media

Jung-Woo Kim,[1] Edmund Perfect,[2] and Heechul Choi[1]

Received 7 February 2006; revised 5 August 2006; accepted 25 August 2006; published 9 January 2007.

[1] Disordered systems are known to induce anomalous diffusion. This phenomenon may be important for environmental applications such as contaminant transport and nutrient availability. However, few studies have investigated anomalous diffusion in this context. In particular, the relationship between pore space geometry and anomalous diffusion is not well understood. We report on numerical simulations of solute diffusion within the water-filled pore spaces of two-dimensional geometrical models of heterogeneous porous media. Euclidean and mass, pore, and pore-solid prefractal lattices were used to generate random pore networks with varying porosity (ϕ) and lacunarity (L). The objectives were to investigate the effects of ϕ and L on the solute random walk dimension (d_w) and to identify which of these models best represents a natural porous medium. Solute diffusion was simulated using a stochastic cellular automaton based on the "myopic ant" algorithm. Estimates of $d_w \gg 2$ occurred with increasing frequency as $\phi \rightarrow 0$, indicating scale dependency in the standard diffusion coefficient at low porosities. The relationship between d_w and ϕ for the mass and pore-solid prefractal lattices was the closest to that for natural 2-D systems (i.e., soil thin sections). The presence of large, interconnected pore spaces ($L \rightarrow 1$) at low porosities reduced the intensity of anomalous diffusion ($d_w \rightarrow 2$). A power law relationship based on the product of d_w and L explained >96% of the total variation in ϕ regardless of the type of lattice considered. The potential predictive capability of this approach for natural porous media deserves further investigation.

Citation: Kim, J.-W., E. Perfect, and H. Choi (2007), Anomalous diffusion in two-dimensional Euclidean and prefractal geometrical models of heterogeneous porous media, *Water Resour. Res.*, *43*, W01405, doi:10.1029/2006WR004951.

1. Introduction

[2] Natural porous media that exhibit significant physical heterogeneities include marine sediments, rocks, saprolite, and soils. In many cases the pore spaces within these Earth materials are completely filled with water. Understanding the diffusion of solutes under saturated conditions is important in environmental applications such as predicting the fate and transport of contaminants, and nutrient availability to plants and microorganisms [*Grathwohl*, 1998; *Tinker and Nye*, 2000].

[3] Diffusion of individual molecules in free space is usually described by the Einstein relation [*Einstein*, 1905], i.e.

$$\langle r^2(t) \rangle \propto t \tag{1}$$

where $\langle r^2(t) \rangle$ is the mean squared displacement at time, t. The constant of proportionality in this linear relationship defines the diffusion coefficient, i.e.

$$D_0 \equiv \frac{\langle r^2(t) \rangle}{t} \tag{2}$$

[4] A large body of theoretical evidence now exists demonstrating that diffusion in model disordered systems deviates from Einstein's classical description and becomes "anomalous" [*Ben-Avraham and Havlin*, 2000]. Examples of such systems include the sample spanning cluster in site percolation models, and the iterative phase in fractal lattices. For these cases, $\langle r^2(t) \rangle$ becomes a nonlinear function of t [*Given and Mandelbrot*, 1983; *Ben-Avraham and Havlin*, 2000]:

$$\langle r^2(t) \rangle \propto t^{d/d_w} \quad (t < t_c) \tag{3a}$$

$$\langle r^2(t) \rangle \propto \lambda \quad (t \geq t_c) \tag{3b}$$

where d is the dimensionality of the system under consideration, d_w is the fractal dimension corresponding to the trail left by a diffusing molecule, λ is the asymptotic value of $\langle r^2(t) \rangle$, and t_c is the critical time at which $\langle r^2(t) \rangle$ reaches λ. As a result, for all times less than the critical time, the diffusion coefficient is no longer a constant, but depends upon the time as:

$$D(t) = D_0 t^{1-d/d_w} \quad (t < t_c) \tag{4}$$

A variety of mathematical techniques, including fractional calculus, are available for incorporating $D(t)$ into a diffusive flux equation analogous to Fick's law [*Metzler and Klafter*, 2000; *Sokolov et al.*, 2002].

[1] Department of Environmental Science and Engineering, Gwangju Institute of Science and Technology, Gwangju, South Korea.
[2] Department of Earth and Planetary Science, University of Tennessee, Knoxville, Tennessee, USA.

0043-1397/07/2006WR004951$09.00

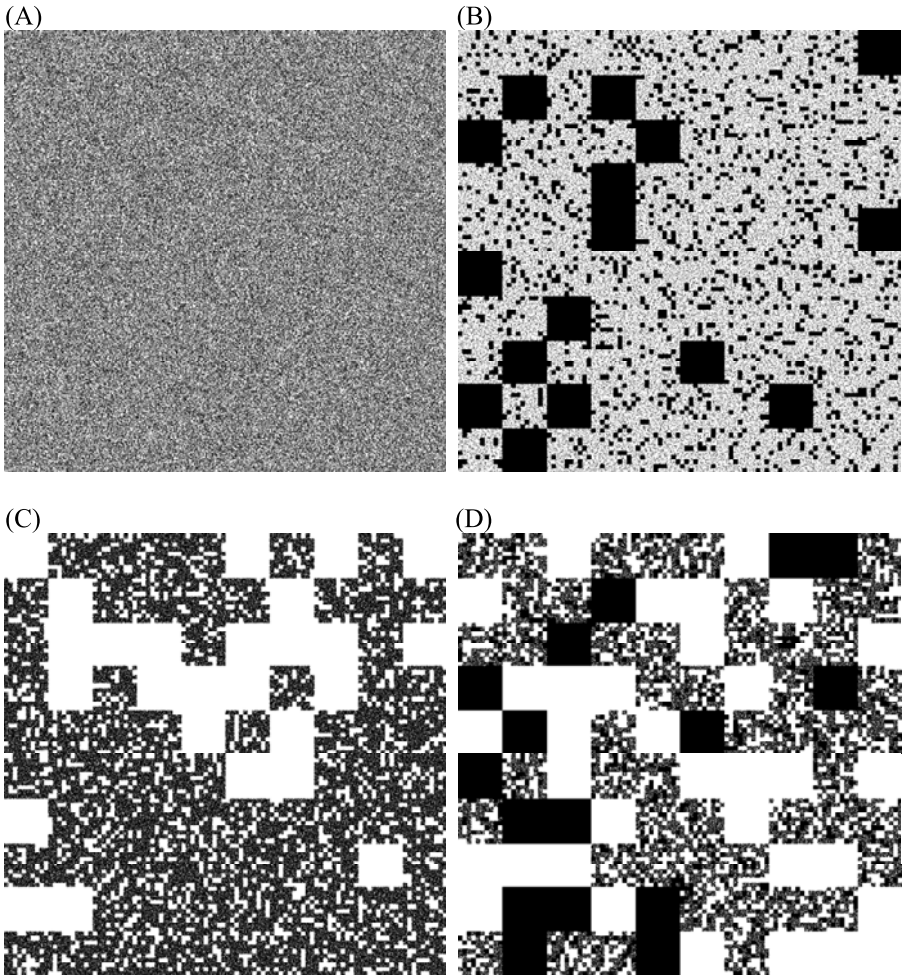

Figure 1. Two-dimensional (a) Euclidean, (b) pore prefractal, (c) mass prefractal, and (d) pore-solid prefractal models of heterogeneous porous media constructed with 10^6 cells and porosities of $\sim$0.6 (white cells, pores; black cells, solids).

[5] While anomalous diffusion in synthetic materials such as catalysts, emulsions, and sorbents is widely accepted [e.g., *Knackstedt et al.*, 1995; *Sheintuch*, 2001; *Malek and Coppens*, 2003], only a few studies have investigated this phenomenon in natural porous media. *Anderson et al.* [1996, 2000] performed numerical random walk simulations in digitized images of thin sections from a wide variety of soil types. Their results indicate that d_w for the pore phase ranges from 2.2 to 2.7. *Ewing and Horton* [2003] studied finite size scaling and edge effects with Monte Carlo simulations in random cubic lattices as models of low-connectivity soils. They showed how the diffusion coefficient deviates from a constant value as porosity decreases. Despite these two reports, the applicability of equation (3) to natural porous media remains to be fully established.

[6] Geometrical models are able to collapse detailed information about complex structures into just a few parameters. By manipulating these parameters in a systematic way, model porous media can be synthesized with a wide range of heterogeneities. Numerical simulations performed within such structures can help identify the respective contributions of different physical properties to anomalous diffusion.

[7] Many different geometrical models have been used to represent natural porous media. A commonly used approach is to randomly assign pores and solids in a Euclidean cubic lattice or site percolation model [*Berkowitz and Ewing*, 1998; *Dullien*, 1992; *Sahimi*, 1995]. Although such models are made up of uniformly sized pore and solid cells (Figure 1a), the pore clusters that occur as the percolation threshold is approached exhibit fractal characteristics. Numerous studies have established the anomalous nature of diffusion in such clusters [*Brandt*, 1975; *de Gennes*, 1976; *Orbach*, 1986]. For two-dimensional Euclidean lattices, the value of d_w for an infinite pore cluster at the percolation threshold is $\sim$2.9 [*Ben-Avraham and Havlin*, 2000].

[8] A major disadvantage of Euclidean lattices as models of natural porous media is that all the pore and solid cells are the same size. Furthermore, heterogeneity is only manifested over a narrow range of porosities close to the percolation threshold. To overcome these limitations various spatially correlated Euclidean models have been proposed [*Duckers*, 1978; *Nauman*, 1993; *Moran and McBratney*, 1997; *Odagaki et al.*, 1999]. According to *Karayiannis et al.* [2001] spatial correlations strongly influence the diffusion process at short times, prolonging

Table 1. Published Estimates of the Random Walk Fractal Dimension, d_w, From Numerical Simulations of Diffusion in Pore Fractal Sierpinski Carpets[a]

	d_w	
Reference	Minimum	Maximum
Kim et al. [1993]	2.07 (1.99)	2.20 (1.72)
Aarão Reis [1995]	2.03 (1.97)	2.12 (1.86)
Aarão Reis [1996a]	2.10 (1.90)	2.49 (1.66)
Aarão Reis [1996b]	2.13 (1.89)	2.25 (1.72)
Dasgupta et al. [1999]	2.19 (1.75)	2.75 (1.75)
Seeger et al. [2001]	2.52 (1.66)	2.71 (1.66)
Tarafdar et al. [2001]	2.45 (1.50)	2.50 (1.50)
Franz et al. [2001]	2.28 (1.75)	2.55 (1.75)
Anh et al. [2005]	2.13 (1.77)	2.60 (1.77)

[a]Fractal dimension, D_f, of the associated Sierpinski carpet is given in parentheses.

the duration of the anomalous regime. While spatially correlated lattices can provide a better representation of heterogeneity, the need for additional empirical parameters in their construction is a potential drawback.

[9] Fractal geometry deals with the scaling of heterogeneous materials. This modeling approach is particularly attractive since information about complexity at different scales is captured in parameters such as the fractal dimension, D_f, and lacunarity, L [*Mandelbrot*, 1982]. Fractal (covering an infinite range of scales) and prefractal (covering a finite range of scales) geometries have been used by many researchers to model natural porous media such as soils and reservoir rocks [*Meakin*, 1991; *Garrison et al.*, 1992; *Adler and Thovert*, 1993; *Rieu and Perrier*, 1998]. These models have been shown to yield theoretical functions for hydraulic properties that closely match experimental data [*Tyler and Wheatcraft*, 1990; *Toledo et al.*, 1990; *Rieu and Sposito*, 1991a, 1991b; *Bird et al.*, 2000; *Perfect*, 2005]. Furthermore, it has long been established that diffusion on fractals is anomalous and can be described by equation (3) [*Gefen et al.*, 1981; *Given and Mandelbrot*, 1983; *Rammal and Toulouse*, 1983].

[10] Fractal porous media can be created by specifying simple rules for interactions between neighboring cells in a lattice (cellular automaton, CA) or by the repeated application of a generator pattern onto itself (iterated function system, IFS). *Crawford et al.* [1997] used the CA approach to simulate aggregated soil structures. Diffusion of solutes within such structures may be normal or anomalous depending upon the interaction rules specified [*Botelho and Aarão Reis*, 1998]. Since CA models are inherently parameterless, however, it is difficult to relate their diffusive behavior to physical properties. In this context, IFS models are preferable.

[11] The focus here is on a special class of two-dimensional IFS fractals known as Sierpinski carpets [*Mandelbrot*, 1982]. A Sierpinski carpet is a pore fractal when the iterative phase is composed solely of voids, a mass fractal when it is composed solely of solids, and a pore-solid fractal when it is composed of both voids and solids [*Perrier et al.*, 1999]. Pore prefractals are made up of different-sized solid particles separated by small uniformly sized pores (Figure 1b). Conversely, mass prefractals consist of different-sized pores and small uniformly sized solid particles (Figure 1c). Pore-solid prefractals contain both solid particle and pore size distributions, and thus are the most physically heterogeneous (Figure 1d). All three types of fractal have been invoked as models of natural porous media [*Katz and Thompson*, 1985; *Garrison et al.*, 1992; *Perrier et al.*, 1999].

[12] Estimates of d_w obtained from numerical simulations of diffusion in pore fractal Sierpinski carpets range from 2.0 to 2.7 (Table 1). To date, no fundamental relationship has been established between d_w and the carpet fractal dimension (D_f). The magnitude of d_w is sensitive to the lattice size [*Aarão Reis*, 1995, 1996a, 1996b], the random walk algorithm [*Seeger et al.*, 2001], and boundary conditions [*Aarão Reis*, 1996a; *Seeger et al.*, 2001]. When these factors are kept constant, d_w generally increases as D_f (and consequently the porosity) decreases [*Aarão Reis*, 1995]. However, for any given carpet dimension, d_w can exhibit significant variation due to differences in pore arrangement and connectivity as quantified by L [*Kim et al.*, 1993; *Dasgupta et al.*, 1999].

[13] Despite the large amount of information available on diffusion in pore prefractal Sierpinski carpets (Table 1), we were unable to locate any published studies dealing with random walk simulations in the void phase of mass and pore-solid Sierpinski carpet fractals. These models are especially relevant to heterogeneous natural porous media since they contain a wide range of pore sizes. The influence of this pore size distribution on their diffusive behavior remains to be elucidated.

[14] This paper reports on numerical simulations of diffusion performed in two-dimensional Euclidean and prefractal lattices, as models of natural porous media. Three classes of prefractals were investigated: pore, mass, and pore-solid Sierpinski carpets. The main objectives were to investigate the effects of varying porosity and lacunarity on the extent of anomalous diffusion in each simulated porous medium, and to relate the results to those obtained by *Anderson et al.* [1996] for soil thin sections. The goal was to identify the best geometrical model for simulating solute diffusion in saturated soil and reservoir rocks.

2. Methods

2.1. Simulated Porous Media

[15] Four different types of two-dimensional model porous media (i.e., Euclidean, pore prefractal, mass prefractal and pore-solid prefractal) were generated (Figure 1). The lattice size was always set at 1000 by 1000 cells in order to compare our results with those from the soil thin section images of *Anderson et al.* [1996] which were 1000 by 1000 pixels.

[16] The Euclidean porous media were generated by the random allocation of pore cells within a solid initiator lattice based on the predetermined porosity.

[17] The prefractal porous media were generated randomly using the homogeneous algorithm [*Sukop et al.*, 2002]. The initiators were pore, solid, and pore-solid lattices in the case of the pore, mass and pore-solid prefractal porous media, respectively. The generators were defined in terms of a constant length subdivision factor (b) and variable predetermined probabilities of exclusion from the generator (p_{ex}) (Table 2). Following subdivision of the initiator and

Table 2. Parameters Used to Generate the Different Prefractal Porous Media With Porosities Ranging From ~0.1 to ~0.6 and a Lattice Size of 1000 × 1000 Cells

Porous Medium	i	b	p_{ex}	ϕ	D_f
Pore prefractal	3	10	0.54	0.0973	1.6628
Pore prefractal	3	10	0.42	0.1951	1.7634
Pore prefractal	3	10	0.33	0.3008	1.8261
Pore prefractal	3	10	0.26	0.4052	1.8692
Pore prefractal	3	10	0.21	0.4930	1.8976
Pore prefractal	3	10	0.16	0.5927	1.9243
Mass prefractal	3	10	0.03	0.0873	1.9868
Mass prefractal	3	10	0.07	0.1956	1.9685
Mass prefractal	3	10	0.11	0.2950	1.9494
Mass prefractal	3	10	0.16	0.4073	1.9243
Mass prefractal	3	10	0.21	0.5070	1.8976
Mass prefractal	3	10	0.26	0.5948	1.8692
Pore-solid prefractal[a]	3	10	0.06	0.1050	1.6990
Pore-solid prefractal[a]	3	10	0.11	0.1925	1.6990
Pore-solid prefractal[a]	3	10	0.17	0.2975	1.6990
Pore-solid prefractal[a]	3	10	0.23	0.4025	1.6990
Pore-solid prefractal[a]	3	10	0.29	0.5075	1.6990
Pore-solid prefractal[a]	3	10	0.34	0.5950	1.6990

[a]Here $p_{gen} = 0.50$.

exclusion of cells, the generators were applied onto themselves in a finite number of iterations (i) (Table 2). In the case of the pore-solid prefractal lattices, only a portion of the remaining generator cells (p_{gen}) was included in the iterative process [*Perrier et al.*, 1999] (Table 2).

2.2. Porosity

[18] The porosity (ϕ) of each porous medium was varied from ~0.1 to ~0.6 in increments of ~0.1 (Table 2). The predetermined ϕ controlled the number of pore cells removed in the Euclidean porous media. The ϕ of each prefractal porous medium was determined by manipulating i, b, p_{ex}, p_{gen}, and the initiator type in the homogeneous algorithm based on the following relations [*Perrier et al.*, 1999; *Sukop et al.*, 2002]:

$$p_{ex} = \frac{n}{b^2} \tag{5a}$$

Pore prefractal

$$\phi = (1 - p_{ex})^i \tag{5b}$$

Mass prefractal

$$\phi = 1 - (1 - p_{ex})^i \tag{5c}$$

Pore-solid prefractal

$$\phi = \frac{p_{ex}}{1 - p_{gen}}\left(1 - p_{gen}^i\right) \tag{5d}$$

where n is the number of cells removed in the generator. In order to maintain a constant lattice size comparable to that of *Anderson et al.*'s [1996] soil thin section images, i and b were fixed at 3 and 10, respectively, and only p_{ex} was varied to control the porosities. In the case of the pore-solid prefractal porous media, p_{gen} was set at a constant value of 0.5 so that variations in porosity were determined exclusively by p_{ex} (Table 2). Five realizations of each type of simulated porous medium were generated at six different porosity levels giving a total of 120 lattices (i.e., 4 models × 6 porosities × 5 replications). Five replications of a 1000 by 1000 free space lattice (i.e., $\phi = 1$) were also included for comparative purposes.

2.3. Pore and Pore Cluster Size Distributions

[19] Both individual pores and pore clusters were accounted for in this study. A pore means a pore cell of a given size that does not include any connected pores. A pore cluster was considered a set of connected pores identified using the Hoshen-Kopelman algorithm [*Hoshen and Kopelman*, 1976]. The Hoshen-Kopelman algorithm was also used to find the largest pore cluster within each realization.

[20] Pore and pore cluster sizes were quantified in terms of their area. The total area of each 1000 by 1000 lattice was set as unity for comparison with the porosity. Thus, for the Euclidean lattices, the pore size was $1/10^6$. For the prefractal lattices, pore sizes were determined using the relationship $1/b^{2j}$ (i.e., $1/10^2$, $1/10^4$, and $1/10^6$ for $j = 1$ to i, respectively). Pore cluster size was calculated as the summed area of the connected pore cells.

2.4. Lacunarity

[21] Generally, knowledge of the porosity is not sufficient to characterize the morphological properties of a porous medium. The spatial distribution of pores can be totally different even though the porosity is constant; for instance, the pores could be either clustered or dispersed. Lacunarity (L) provides a quantitative measure of the spatial distribution of pores within a porous medium [*Pendelton et al.*, 2005]. In this study, L was calculated based on the pores and pore clusters within each lattice using the method suggested by *Allain and Cloitre* [1991]:

$$L = \frac{\sum_p p^2 Q(p,r)}{\left(\sum_p pQ(p,r)\right)^2} \tag{6}$$

where p is the number of pore cells in a gliding window whose size (area) is r, and $Q(p, r)$ is the probability function of the pore distribution. Equation (6) corresponds to the ratio between the second moment and the square of the first moment of the pore space distribution. Consequently, the greater the degree of pore cell coalescence, the higher the value of L.

[22] The L of a lattice has upper and lower bounding values depending upon the size of the gliding window selected: $L \to 1$ as r approaches the area of the entire lattice, while $L \to 1/\phi$ as r approaches the cell or pixel area. For prefractal lattices, differences in L due to pore clustering appear to be most pronounced when $r = b^{-(2i-1)}$ [*Turcotte*, 1997]. Thus, in this study the area of the gliding window was set at $1/10^5$.

2.5. Solute Diffusion

[23] Solute diffusion was simulated with multiple random walkers or particles using the myopic ant algorithm [*Ben-Avraham and Havlin*, 2000]. In order to quantify only the effects of pore space geometry on solute diffusion, the

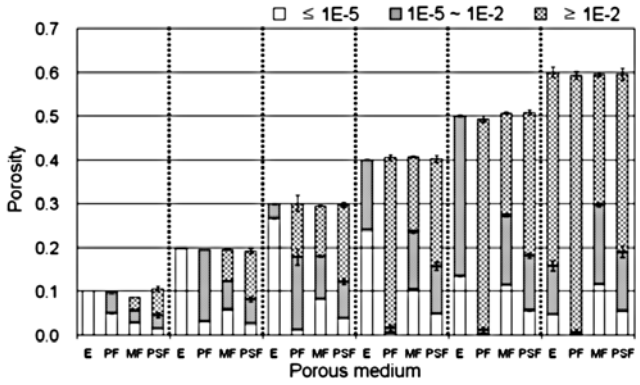

Figure 2. Sums of pore clusters with sizes less than 10^{-5} (white), between 10^{-5} and 10^{-2} (shaded), and more than 10^{-2} (stippled) for each porosity level in each porous medium (E, Euclidean; PF, pore prefractal; MF, mass prefractal; PSF, pore-solid prefractal). Vertical error bars indicate ±95% CI for each pore cluster size class.

cloud of solute particles was considered to be an inert tracer (i.e., no interactions between solute particles or with the solid phase). One hundred solute particles were initially distributed within the pore phase of each simulated porous medium. Because the particles were randomly inserted, some of them ended up being trapped in isolated pores. Since the particles do not "see" one another it was possible for more than one particle to occupy the same cell at the same time. Additional simulations in Euclidean porous media at two porosities above and below the percolation threshold (ϕ = 0.6 and 0.4, respectively) using 1000 solute particles were consistent with those obtained using just 100 solute particles (data not presented).

[24] Incremental particle movements were restricted to the von Neumann neighborhood, which comprises the four closest cells. An equal probability of movement to each neighboring pore cell was employed. If one or more neighboring cells were solids, then the probability was reequalized for the remaining pore neighbors. If all of the neighbors were solids, the probability of the solute particle movement was zero. The total diffusion simulation time in each porous medium was set at 1000 incremental steps. This value was chosen because $\langle r^2(t)\rangle$ became steady after ~1000 time steps, which is consistent with the results of *Ben-Avraham and Havlin* [2000]. There were no differences in the simulations when 3000 times steps was used instead of 1000 time steps in Euclidean porous media at ϕ = 0.6 and 0.4 (data not presented).

[25] At each time step (t), the $\langle r^2(t)\rangle$ was computed for the 100 solutes, synchronously. In order to represent an infinite system, periodic boundary conditions were adopted for all four edges of the model domain. This means that when a solute particle exited from one side of the lattice, the particle was reintroduced on the opposite side of the lattice at the same time. We also simulated anomalous diffusion in 256 × 256 sized Euclidean lattices at ϕ = 0.6 and 0.4 for comparison. The results (not shown) indicated there were no significant differences due to the lattice size. This suggests that the periodic boundary condition was effective in reducing the impact of finite size effects.

[26] In order to quantify solute diffusion in the simulated porous media, equation (3) was fitted to the mean squared displacement versus time data from the random walks with d set at 2. The d_w and λ parameters were estimated by segmented nonlinear regression analysis using the SAS statistical software program [*SAS Institute Inc.*, 1999], with the critical time separating the two diffusive modes defined by:

$$t_c = \lambda^{d_w/2} \tag{7}$$

Estimates of $t_c > 1000$ occurred in 29%, 40%, 43%, and 50% of the fits for the Euclidean, pore prefractal, mass prefractal, and pore-solid prefractal porous media, respectively. In these cases the data were refitted using only equation (3a). With the exception of the Euclidean lattices the occurrence of $t_c > 1000$ appeared to be independent of the porosity. For the former, the percentage of cases in which $t_c > 1000$ decreased systematically with decreasing porosity.

[27] While convergence was always achieved according to the SAS software default criterion, equation (3) did not always provide a good fit to the data, particularly in the case of the Euclidean and pore prefractal lattices with very low porosities. Altogether 22% of the 125 fits were excluded from further analysis because their coefficients of determination (R^2) between the observed and predicted values were less than 0.9. Mean values and associated 95% confidence intervals (CI) for d_w were computed based on the remaining fits for the five different realizations at each porosity in each type of simulated porous medium.

3. Results and Discussion

3.1. Pore and Pore Cluster Size Distributions

[28] The main morphological differences between the four types of simulated porous media (Figure 1) can be attributed to their pore and pore cluster size distributions. In the Euclidean and pore prefractal porous media only the smallest lattice cells ($1/10^6$) were present as pores. As a result their pore size distributions were uniform. In the mass and pore-solid prefractal porous media, however, three different pore sizes were present, corresponding to the iteration level in the relationship between b and i.

[29] Because of the definition of pore size, and the fact that the homogeneous algorithm was used to construct the prefractal porous media, there was no variation in the pore size distributions among the different replications. In contrast, the pore cluster size distributions showed small variations between the different realizations as indicated by the 95% CI in Figure 2. The pore cluster size distributions were highly dependent upon both the type of porous medium and the porosity (Figure 2). In the Euclidean and pore prefractal porous media, especially, the pore cluster size distributions changed dramatically as the porosity increased. This observation is consistent with percolation threshold theory which, in the case of Euclidean porous media, predicts the occurrence of a sample spanning pore cluster at ϕ = 0.5927... [*Ben-Avraham and Havlin*, 2000]. For the mass and pore-solid prefractal porous media the relative proportions of pore clusters in each size class did not change as much as the porosity increased (Figure 2).

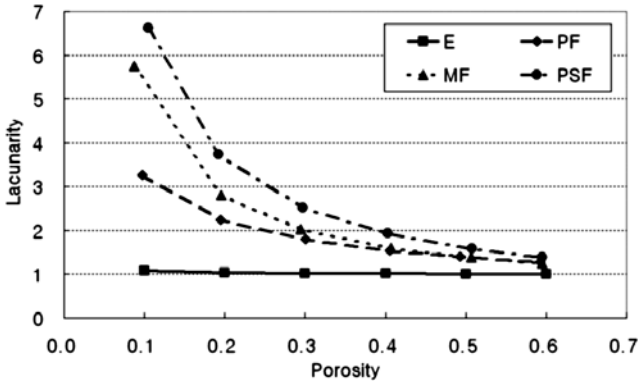

Figure 3. Lacunarity as a function of porosity for each porous medium (E, Euclidean; PF, pore prefractal; MF, mass prefractal; PSF, pore-solid prefractal). Note that ±95% CI were smaller than the data points.

However, the largest pore clusters always occupied a greater fraction of the total pore space than the largest pores.

3.2. Lacunarity

[30] The effects of porosity and type of porous medium on the L parameter were very clear since there was little variation between the replications as evidenced by the negligibly small 95% CI in Figure 3. The effect of type of porous medium on L was strongly dependent on the porosity. At low porosities, there were highly significant differences in L between the different porous media, whereas at high porosities the differences were less pronounced. This is to be expected since fewer and fewer solid cells occur as $\phi \rightarrow 1$, so that there is insufficient information for equation (6) to quantify pore coalescence. This occurs regardless of the nature of the pore cell size distribution. In contrast, at low porosities many solid cells are present so that pore cell clusters are easily distinguished from dispersed/isolated pore cells.

[31] The influence of a solid (particle) cell size distribution versus a uniform particle cell size can be seen by comparing the L versus ϕ functions for the pore prefractal and Euclidean porous media (both systems had a uniform pore cell size). Similarly, the influence of a pore cell size distribution versus a uniform pore cell size can be seen by contrasting the L versus ϕ functions for the mass prefractal and Euclidean porous media (both systems had a uniform particle size). This comparison (Figure 3) indicates that at low porosities L is much more sensitive to the presence of large pores than large particles. The pore-solid prefractal porous media contained both pore and particle cell size distributions and, as a result, produced the strongest relationship between L and ϕ (Figure 3). Apparently, the presence of large particles at low porosities enforces additional pore clustering as compared to that associated with just a pore cell size distribution (i.e., the mass prefractal model).

3.3. Mean Squared Displacement

[32] The mean squared displacement versus time functions varied with both the type of porous medium and the porosity (Figure 4). Generally, $\langle r^2(t) \rangle$ has a linear relationship with time in open space. However, when particle movement is constrained by the solid phase, diffusion becomes increasingly anomalous [*Ben-Avraham and Havlin*, 2000].

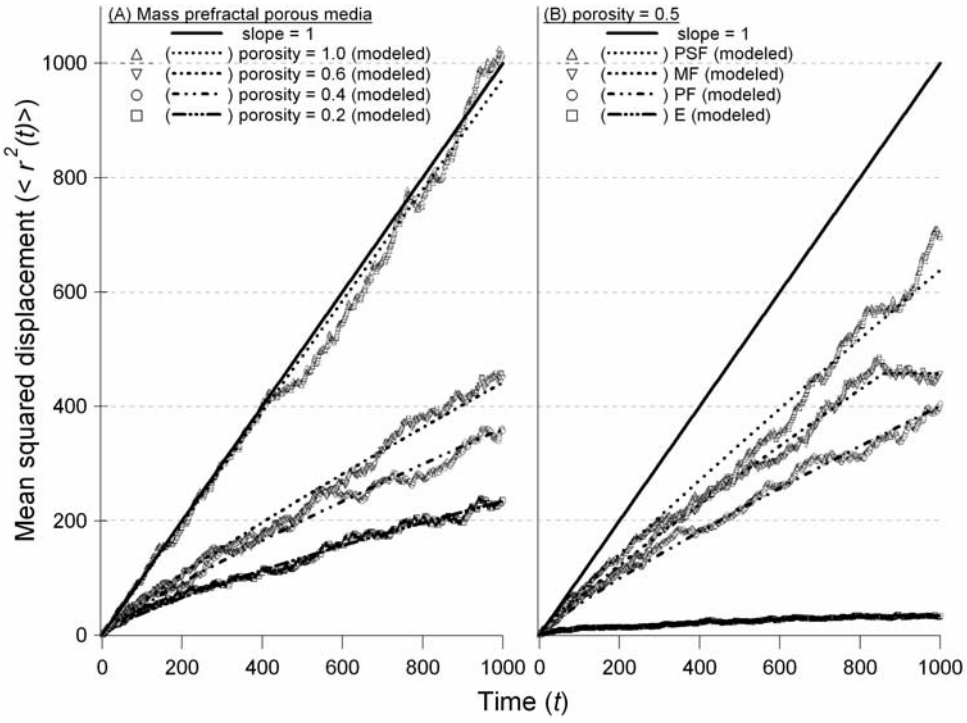

Figure 4. Mean squared displacement versus time functions for inert solute particles (a) in mass prefractal porous media with porosities of 0.2, 0.4, 0.6 and 1.0 and (b) in different porous media (E, Euclidean; PF, pore prefractal; MF, mass prefractal; PSF, pore-solid prefractal) where porosity = 0.5 (symbols, experimental results; lines, modeled results).

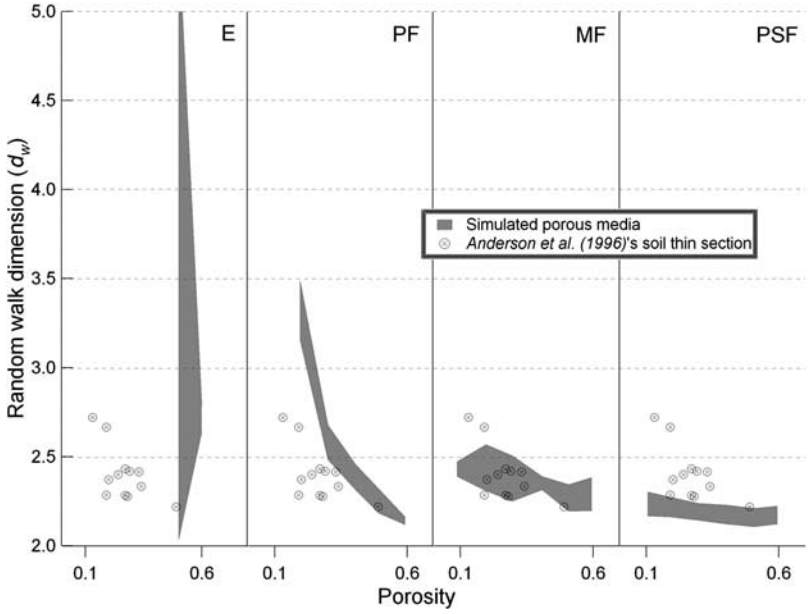

Figure 5. Random walk dimension as a function of porosity in each porous medium (E, Euclidean; PF, pore prefractal; MF, mass prefractal; PSF, pore-solid prefractal porous media) as compared to *Anderson et al.*'s [1996] results for soil thin sections (circled crosses). The shaded regions indicate the ±95% CI.

Figure 4a shows the mean squared displacement versus time functions for open space and the mass prefractal porous media at selected porosities. As expected, the $\langle r^2(t)\rangle$ versus t relations were approximately linear when $\phi = 1$. Regardless of the porous medium considered, the functions became increasingly curvilinear and asymptotic at earlier times (i.e., more anomalous) as porosity decreased. This is because the pore clusters, in which solute diffusion occurs, are smaller and more convoluted at low porosity, so the space available for solute movements is limited.

[33] For any given porosity, the type of porous medium also affected the degree of anomalous behavior (Figure 4b). The Euclidean porous media always produced the most anomalous diffusion, followed by the pore prefractal porous media. In contrast, the mass and pore-solid prefractal porous media, which had one or more large pores present, generally yielded more linear and less asymptotic mean squared displacement versus time functions.

3.4. Effects of Porous Medium and Porosity on Random Walk Dimension

[34] Our random walk algorithm was verified by performing replicated solute diffusion simulations in free space (i.e., $\phi = 1$). The mean value of the resulting d_w estimates (2.01 ± 0.02) was not significantly different from the theoretical value of two at $p < 0.05$.

[35] For the simulated porous media, estimates of d_w always increased as the porosity decreased (Figure 5). The Euclidean and pore prefractal porous media exhibited very large increases in d_w with decreasing porosity because of the dramatic changes in their pore cluster size distributions. Compared to *Anderson et al.*'s [1996] soil thin section data, the d_w values for the Euclidean and pore prefractal porous media were overestimated, especially at low porosities. In contrast, Figure 5 indicates that the mass and pore-solid prefractal porous media, both which had hierarchical pore cell and pore cluster size distributions, displayed much less variation in d_w. This result suggests that mass and pore-solid prefractals can be regarded as the closest geometrical model to real soil among the four simulated porous media investigated.

[36] Although the mass prefractals gave the best overall match with the soil thin section data, it is not possible to conclude that this model was better than the pore-solid prefractal model. This is because only one value of p_{gen} was used in the construction of the pore-solid prefractals, and it is possible that a closer fit to the soil thin section data might be obtained by varying this parameter. Additional simulations in pore-solid prefractal porous media are needed to more fully elucidate the nature of the relationship between p_{gen} and d_w.

[37] The random walkers were free to move throughout the pore clusters in each porous medium. However, their mean squared displacements were highly restricted in the smallest pore clusters, as demonstrated by the high values of d_w and small pore cluster sizes at low porosities in the Euclidean and pore prefractal porous media. On the other hand, the mass and pore-solid prefractal porous media always had some large pores present even at low porosities, resulting in relatively low values of d_w. These results suggest that both pore cell and pore cluster size are important factors controlling the extent of anomalous diffusion within water-saturated porous media.

[38] For the Euclidean porous media with a porosity of 0.6, the proportions of large pore clusters were similar to, or higher than, the proportions present in the mass and pore-solid prefractal porous media. In addition, the lacunarity values were similar when porosity is about 0.6. Thus one might have expected similar, or lower, d_w values. However, the d_w values for the Euclidean porous media were higher than those for the mass and pore-solid prefractal porous media. Considering pore size distribution, the Euclidean porous media had uniformly small pore sizes even at high

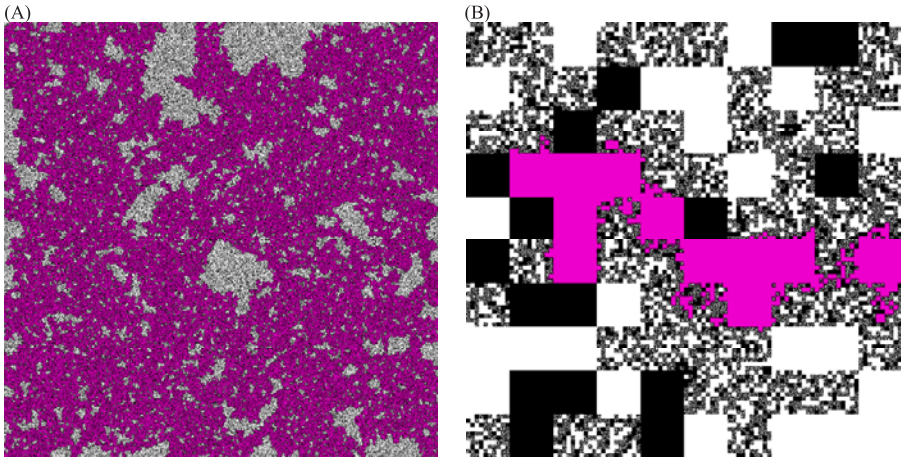

Figure 6. Largest pore clusters in (a) Euclidean and (b) pore-solid prefractal porous media with porosities of ~0.6 (white, pore; black, solid; purple, largest pore cluster).

porosity. However, the pore cluster sizes were much larger than those in the other media (Figure 2). In other words, although the pore cluster size was very large, its morphology was more disordered, with less dense pore cells and more dangling ends. In contrast, the mass and pore-solid prefractals had pore clusters that included large pore cells (macropores) which were very similar to open space. These differences in pore cluster morphology are illustrated in Figure 6.

3.5. Integrated Model for Anomalous Diffusion

[39] Comparing our results from Figures 3 and 5, it can be seen that the relationship between lacunarity and the random walk dimension depends upon the porosity level considered. At high ϕ there was no clear relationship between d_w and L. In contrast, at low ϕ, the d_w increased as the L decreased. This relationship is as expected, since a high lacunarity value corresponds to greater degree of pore coalescence, which should diminish the overall extent of anomalous diffusion.

[40] The interaction between L and ϕ indicates that anomalous diffusion is significantly influenced by, not only porosity, but also the type of porous medium. When these parameters were multiplied together, however, the porous medium effect was removed (Figure 7). The combined variation of L and d_w with porosity can be explained by the following generic power law relationship:

$$d_w \times L = f(\phi) = \alpha \times \phi^{-\beta} \tag{8}$$

From physical considerations, both L and d_w are expected to go to infinity as porosity goes to zero. In addition, L should

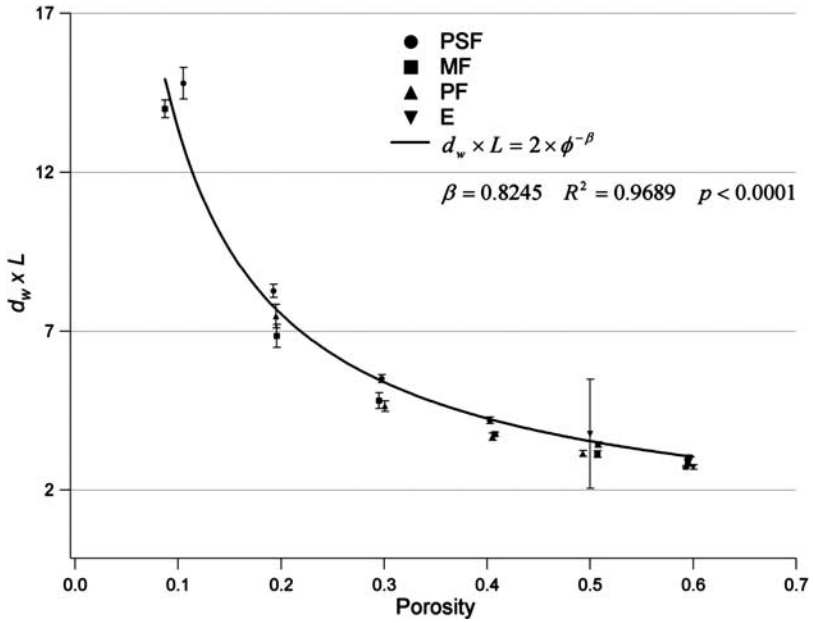

Figure 7. Mean values (±95% CI) of $d_w \times L$ for each porous medium (E, Euclidean; PF, pore prefractal; MF, mass prefractal; PSF, pore-solid prefractal) as a function of porosity. The best fit relationship based on equation (8) with $\alpha = 2$ is shown as a solid line along with the calculated parameter and coefficient of determination (R^2).

go to one and d_w to two as the porosity approaches unity (see Figures 3 and 5). On the basis of the above boundary conditions α was fixed as a constant of two and β was estimated from the data using nonlinear regression in SAS ($R^2 = 0.9689$, $p < 0.0001$). Given these results, equation (8) can be rewritten as

$$d_w \times L = 2 \times \phi^{-0.8245} \quad (9)$$

The physical significance and potential universality of the power exponent in equation (9) will require further investigation in future studies.

[41] Equation (9) suggests that a combination of d_w, which is a characteristic of anomalous diffusion, and L, which is a morphological property of porous media, can be estimated by porosity no matter which type of porous medium is considered. Further research with digitized images of soil and rock thin sections is needed to test the applicability of this relationship to natural porous media (unfortunately, *Anderson et al.*'s [1996] original images were not available for analysis). Extension of the current work to three dimensions would also be valuable.

4. Conclusions

[42] Anomalous diffusion was investigated in simulated porous media. In order to realize the heterogeneous geometry of natural porous media, three different prefractal porous media (pore, mass, and pore-solid prefractals) were employed and compared with random Euclidean porous media. Differences in pore space geometry within the porous media could be clearly discriminated based upon the measured pore cell and pore cluster size distributions. Lacunarity proved to be a powerful parameter for quantifying these differences. Solute diffusion within the pore spaces of the model porous media was simulated using the myopic ant algorithm. The mean squared displacements of the random walkers (solute particles) were influenced by the pore and pore cluster size distributions, as well as by total porosity. On the basis of our results, it can be concluded that anomalous behavior increases with decreasing pore cell and pore cluster size and uniformity, as well as with decreasing porosity. Heterogeneous pore clusters which contain macropores are similar in effect to open space and diminish the overall extent of anomalous diffusion. Regardless of the type of porous medium considered, a power law relationship based on porosity explained >96% of the total variation observed in the random walk dimension of the solute particles multiplied by lacunarity. Comparing our results to those from soil thin sections, suggests that mass and pore-solid prefractal lattices can be regarded as the most applicable geometrical models for simulating solute diffusion in natural porous media.

[43] **Acknowledgments.** This research was supported by a grant (4-1-2) from Sustainable Water Resource Research Center (SWRRC) of 21st century frontier R&D program and by Research Funds of the National Research Laboratory Program (project M10500000128-05J0000-12810) from the Ministry of Science and Technology in South Korea through the Center for Water Research (CWR) at Gwangju Institute of Science and Technology (GIST).

References

Aarão Reis, F. D. A. (1995), Finite-size scaling for random walks on fractals, *J. Phys. A Math. Gen.*, *28*, 6277–6287.

Aarão Reis, F. D. A. (1996a), Scaling for random walks on Sierpinski carpets, *Phys. Lett. A*, *214*, 239–242.

Aarão Reis, F. D. A. (1996b), Diffusion on regular random fractals, *J. Phys. A Math. Gen.*, *29*, 7803–7810.

Adler, P. M., and J.-F. Thovert (1993), Fractal porous media, *Transp. Porous Media*, *13*, 41–78.

Allain, C., and M. Cloitre (1991), Characterizing the lacunarity of random and deterministic fractal sets, *Phys. Rev. A*, *44*, 3552–3558.

Anderson, A. N., A. B. McBratney, and E. A. FitzPatrick (1996), Soil mass, surface, and spectral fractal dimensions estimated from thin section photographs, *Soil Sci. Soc. Am. J.*, *60*, 962–969.

Anderson, A. N., J. W. Crawford, and A. B. McBratney (2000), On diffusion in fractal soil structures, *Soil Sci. Soc. Am. J.*, *64*, 19–24.

Anh, D. H. N., K. H. Hoffmann, S. Seeger, and S. Tarafdar (2005), Diffusion in disordered fractals, *Europhys. Lett.*, *70*, 109–115.

Ben-Avraham, D., and S. Havlin (2000), *Diffusion and Reactions in Fractals and Disordered Systems*, Cambridge Univ. Press, New York.

Berkowitz, B., and R. P. Ewing (1998), Percolation theory and network modeling applications in soil physics, *Surv. Geophys.*, *19*, 23–72.

Bird, N. R. A., E. Perrier, and M. Rieu (2000), The water retention function for a model of soil structure with pore and solid fractal distributions, *Eur. J. Soil Sci.*, *51*, 55–63.

Botelho, S. S., and F. D. A. Aarão Reis (1998), Diffusion on complex automata patterns, *Physica A*, *260*, 338–348.

Brandt, W. W. (1975), Use of percolation theory to estimate effective diffusion coefficients of particles on various ordered lattices and a random network structure, *J. Chem. Phys.*, *63*, 5162–5167.

Crawford, J. W., S. Verrall, and I. M. Young (1997), The origin and loss of fractal scaling in simulated soil aggregates, *Eur. J. Soil Sci.*, *48*, 643–650.

Dasgupta, R., T. K. Ballabh, and S. Tarafdar (1999), Scaling exponents for random walks on Sierpinski carpets and number of distinct sites visited: A new algorithm for infinite fractal lattices, *J. Phys. A Math. Gen.*, *32*, 6503–6516.

de Gennes, P. G. (1976), Relation between percolation theory and elasticity of gels, *J. Phys. Paris*, *37*, L1–L2.

Duckers, L. J. (1978), Percolation with nearest neighbor interaction, *Phys. Lett. A*, *67*, 93–94.

Dullien, F. A. L. (1992), *Porous Media: Fluid Transport and Pore Structure*, 2nd ed., Elsevier, New York.

Einstein, A. (1905), On the movement of small particles suspended in stationary liquids required by the molecular-kinetic theory of heat, *Ann. Phys.*, *17*, 549–560.

Ewing, R. P., and R. Horton (2003), Diffusion scaling in low connectivity porous media, in *Scaling Methods in Soil Physics*, edited by Y. Pachepsky et al., pp. 49–61, CRC Press, Boca Raton, Fla.

Franz, A., C. Schulzky, S. Tarafdar, and K. H. Hoffmann (2001), The pore structure of Sierpinski carpets, *J. Phys. A Math. Gen.*, *34*, 8751–8765.

Garrison, J. R., Jr., W. C. Pearn, and D. U. von Rosenberg (1992), The fractal Menger sponge and Sierpinski carpet as models for reservoir rock/pore systems: I. Theory and image analysis of Sierpinski carpets, *In Situ*, *16*, 351–406.

Gefen, Y., A. Aharony, B. B. Mandelbrot, and S. Kirkpatrick (1981), Solvable fractal family and its possible relation to the backbone at percolation, *Phys. Rev. Lett.*, *47*, 1771–1774.

Given, J. A., and B. B. Mandelbrot (1983), Diffusion and fractal lattices and fractal Einstein relation, *J. Phys. A Math. Gen.*, *16*, L565–L569.

Grathwohl, P. (1998), *Topics in Environmental Fluid Mechanics*, vol. 1, *Diffusion in Natural Porous Media*, Springer, New York.

Hoshen, J., and R. Kopelman (1976), Percolation and cluster distribution. I. Cluster multiple labeling technique and critical concentration algorithm, *Phys. Rev. B*, *14*, 3438–3445.

Karayiannis, N. C., V. G. Mavrantzas, and D. N. Theodorou (2001), Diffusion of small molecules in disordered media: Study of the effect of kinetic and spatial heterogeneities, *Chem. Eng. Sci.*, *56*, 2789–2801.

Katz, A. J., and A. H. Thompson (1985), Fractal sandstone pores: Implications for conductivity and pore formation, *Phys. Rev. Lett.*, *54*, 1325–1328.

Kim, M. H., D. H. Kim, and I.-M. Kim (1993), Lower and upper bounds for the anomalous diffusion exponent on Sierpinski carpets, *J. Phys. A Math. Gen.*, *26*, 5655–5660.

Knackstedt, M. A., B. W. Ninham, and M. Monduzzi (1995), Diffusion in model disordered media, *Phys. Rev. Lett.*, *75*, 653–656.

Malek, K., and M.-O. Coppens (2003), Knudsen self- and Fickian diffusion in rough nanoporous media, *J. Chem. Phys.*, *119*, 2801–2811.

Mandelbrot, B. B. (1982), *The Fractal Geometry of Nature*, W. H. Freeman, New York.

Meakin, P. (1991), Fractal aggregates in geophysics, *Rev. Geophys.*, *29*, 317–354.

Metzler, R., and J. Klafter (2000), The random walk's guide to anomalous diffusion: A fractional dynamics approach, *Phys. Rep.*, *339*, 1–77.

Moran, C. J., and A. B. McBratney (1997), A two-dimensional fuzzy random model of soil pore structure, *Math. Geol.*, *29*, 755–777.

Nauman, E. B. (1993), Cocontinuity and percolation in correlated structures, *AIChE Symp. Ser.*, *89*, 134–142.

Odagaki, T., H. Kawai, and S. Toyofuku (1999), Percolation in correlated systems, *Physica A*, *266*, 49–54.

Orbach, R. (1986), Dynamics of fractal networks, *Science*, *231*, 814–819.

Pendelton, D. E., A. Dathe, and P. Baveye (2005), Influence of image resolution and evaluation algorithm on estimates of the lacunarity of porous media, *Phys. Rev. E*, *72*(4), 041306, doi:10.1103/PhysRevE.72.041306.

Perfect, E. (2005), Modeling the primary drainage curve of prefractal porous media, *Vadose Zone J.*, *4*, 959–966.

Perrier, E., N. R. A. Bird, and M. Rieu (1999), Generalizing the fractal model of soil structure: The pore-solid fractal approach, *Geoderma*, *88*, 137–164.

Rammal, R., and G. Toulouse (1983), Random walks on fractal structures and percolation clusters, *J. Phys. Paris*, *44*, L14–L22.

Rieu, M., and E. Perrier (1998), Fractal models of fragmented and aggregated soils, in *Fractals in Soil Science*, *Dev. Soil Sci. Ser.*, vol. 27, edited by P. Baveye et al., pp. 169–202, CRC Press, Boca Raton, Fla.

Rieu, M., and G. Sposito (1991a), Fractal fragmentation, soil porosity, and soil water properties: I. Theory, *Soil Sci. Soc. Am. J.*, *55*, 1231–1238.

Rieu, M., and G. Sposito (1991b), Fractal fragmentation, soil porosity, and soil water properties: II. Applications, *Soil Sci. Soc. Am. J.*, *55*, 1239–1244.

Sahimi, M. (1995), *Flow and Transport in Porous Media and Fractured Rock*, John Wiley, Hoboken, N. J.

SAS Institute Inc. (1999), *SAS/STAT® User's Guide*, *Version 8*, Cary, N. C.

Seeger, S., A. Franz, C. Schulzky, and K. H. Hoffmann (2001), Random walks on finitely ramified Sierpinski carpets, *Comput. Phys. Commun.*, *134*, 307–316.

Sheintuch, M. (2001), Reaction engineering principles of processes catalyzed by fractal solids, *Catal. Rev. Sci. Eng.*, *43*, 233–289.

Sokolov, I. M., J. Klafter, and A. Blumen (2002), Fractional kinetics, *Phys. Today*, *55*, 48–54.

Sukop, M. C., G.-J. van Dijk, E. Perfect, and W. K. P. van Loon (2002), Percolation thresholds in 2-dimensional prefractal models of porous media, *Transp. Porous Media*, *48*, 187–208.

Tarafdar, S., A. Franz, C. Schulzky, and K. H. Hoffmann (2001), Modelling porous structures by repeated Sierpinski carpets, *Physica A*, *292*, 1–8.

Tinker, P. B., and P. H. Nye (2000), *Solute Movement in the Rhizosphere*, Oxford Univ. Press, New York.

Toledo, P. G., R. A. Novy, H. T. Davis, and L. E. Scriven (1990), Hydraulic conductivity of porous media at low water content, *Soil Sci. Soc. Am. J.*, *54*, 673–679.

Turcotte, D. L. (1997), *Fractals and Chaos in Geology and Geophysics*, 2nd ed., Cambridge Univ. Press, New York.

Tyler, S., and S. W. Wheatcraft (1990), Fractal processes in soil water retention, *Water Resour. Res.*, *26*, 1047–1054.

H. Choi and J.-W. Kim, Department of Environmental Science and Engineering, GIST, Gwangju 500-712, South Korea. (hcchoi@gist.ac.kr; jwookim@gist.ac.kr)

E. Perfect, Department of Earth and Planetary Science, University of Tennessee, Knoxville, TN 37996, USA. (eperfect@utk.edu)